HHS Public Access

Author manuscript

J Biomed Nanotechnol. Author manuscript; available in PMC 2015 October 28.

Published in final edited form as:

J Biomed Nanotechnol. 2015 October ; 11(10): 1722–1733.

Therapeutical Neurotargeting via Magnetic Nanocarrier: Implications to Opiate-Induced Neuropathogenesis and NeuroAIDS

Vidya Sagar[*], **Sudheesh Pilakka-Kanthikeel**, **Venkata S. R. Atluri**, **Hong Ding**, **Adriana Y. Arias**, **Rahul D. Jayant**, **Ajeet Kaushik**, and **Madhavan Nair**[*]

Center for Personalized Nanomedicine/Institute of NeuroImmune Pharmacology, Department of Immunology, Herbert Wertheim College of Medicine, Florida International University, Miami, 33199, FL

Abstract

Magnetite (Fe_3O_4) is the most commonly and extensively explored magnetic nanoparticles (MNPs) for drug-targeting and imaging in the field of biomedicine. Nevertheless, its potential application as safe and effective drug-carrier for CNS (Central Nervous System) anomalies is very limited. Previous studies have shown an entangled epidemic of opioid use and HIV infection and increased neuropathogenesis. Opiate such as morphine, heroine, etc. are used frequently as recreational drugs. Existing treatments to alleviate the action of opioid are less effective at CNS level due to impermeability of therapeutic molecules across brain barriers. Thus, development of an advanced nanomedicine based approach may pave the way for better treatment strategies. We herein report magnetic nanoformulation of a highly selective and potent morphine antagonist, CTOP (D-Pen-Cys-Tyr-DTrp-Orn-Thr-Pen-Thr-NH_2), which is impenetrable to the brain. MNPs, synthesized in size range from 25 to 40 nm, were characterized by Transmission electron microscopy and assembly of MNPs-CTOP nanoformulations were confirmed by FTIR spectroscopy and fluorescent detection. Flow-cytometry analysis showed that biological efficacy of this nanoformulation in prevention of morphine induced apoptosis in peripheral blood mononuclear cells remains equivalent to that of free CTOP. Similarly, confocal microscopy reveals comparable efficacy of free and MNPs bound CTOP in protecting modulation of neuronal dendrite and spine morphology during morphine exposure and morphine-treated HIV infection. Further, typical transmigration assay showed increased translocation of MNPs across *in vitro* blood-brain barrier upon exposure of external magnetic force where barrier integrity remains unaltered. Thus, the developed nanoformulation could be effective in targeting brain by application of external magnetic force to treat morphine addiction in HIV patients.

Keywords

Magnetic Nanoparticles; Morphine; HIV; Neuropathogenesis; Blood-Brain Barrier (BBB)

[*]Authors to whom correspondence should be addressed. nairm@fiu.edu, vsaga001@fiu.edu.

INTRODUCTION

Recreational drugs and HIV have many common mechanisms and sites of action in brain. As such, recreational drugs exposure aggravates HIV neuropathogenesis (neuroAIDS). Also, drug addiction and subsequent psychological emotions result in therapeutical non-adherence in many cases causing intensification of disease. Particularly, in HIV infection—where about one-tenth of population is drug abuser—therapeutics non-adherence has been categorized as a major impediment towards AIDS prevention. Therefore, incorporation of anti-addiction agents in treatment strategies of many diseases, including anti-HIV therapy (HAART), is the important health priority. Currently more than 230 million people around the globe are illicit drug users. Opiates—morphine and heroine— are among most popular recreational drugs and account for 26–36 million users globally.[1] Among other recreational drugs, opiates, alone or during HIV infection, also have been shown to alter the neuroplasticity resulting in various neurological abnormalities.[2–4] Opiates disrupt the dopaminergic function in nervous system which leads to neuro-immunological compromise and subsequently enhances proinflammatory production and exacerbates neuronal cells inflammation.[5–8] Opioid-mediated neuro-immunological alteration increases HIV neuroinvasiveness and weakens the nervous system ability to respond against HIV neurovirulence causing additive stimulation in HIV-associated neurocognitive disorders.[5–9] Opiates primarily exert its effect via μ-opioid receptors and as such, a selective antagonist of this receptor, namely CTOP (D-Pen-Cys-Tyr-DTrp-Orn-Thr-Pen-Thr-NH_2), counterchecks their detrimental consequences. Nevertheless, CTOP does not transmigrate across blood-brain barrier (BBB) and, in turn, leaves little space for opioid's addiction therapy. In fact more than 99% of drugs are impermeable to BBB providing little or no benefit for most brain diseases. Hence, successful drug delivery in brain requires improvement over existing technologies.

Use of nanotechnology in medicine has shown exiting prospect for development of novel drug delivery systems. However, existing nanovehicles such as liposomes, dendrimers, polymers, micelles, solid-lipid nanoparticles etc. have one or more major limitations that affect their BBB transmigration ability. Primarily, after systemic administration these nanocarriers remain in the peripheral circulation for long time and, in turn, engulfed by the reticuloendothelial systems (RES) before reaching to BBB. Thus uncertainty—if and when nanocarrier reaches brain—always persist. So, effective drugs targeting in brain requires speedy systemic transport of carriers to the BBB such that they get little exposure to the RES. Recently magnetic (magnetite–Fe_3O_4) nanoparticle (MNP) has gained significant attention and been intensively investigated for their biomedical applications ranging from imaging to drug targeting. MNPs possess distinct advantage over abovementioned counterparts in that its inherent superparamagnetism allow control over its magnetization—and so over its movement/speed—by external magnetic field.[10–13] Thus, MNP's tissue-specific targeting and distribution can be managed remotely by applying non-invasive magnetic force of required intensity at the desired site. Nonetheless, MNPs application as targeted and safe drug carrier is primarily limited to peripheral organs and, despite being a crucial agent for brain MRI (magnetic resonance imaging), its applications for CNS drug delivery has been little explored. We hypothesize that CTOP molecules immobilized on the

MNPs can be delivered across the blood-brain barrier under the influence of external magnetic force in more faster and effective manner leading the way for neutralization of opiate-induced neuropathogenesis and neuroAIDS. Accordingly, we characterized the zeta potential of MNPs and evaluated the MNPs-CTOP binding isotherm, their pharmacokinetics, peripheral and neuronal functional efficacy, and toxicity. Herein, for the first time, we report that MNPs can be a potential platform for direct nanodelivery of CTOP in brain to countercheck the additive neuronal injury by morphine during HIV infection. We believe that this novel therapeutical approach may have universal applicability against varieties of CNS diseases which includes treatment of other recreational drugs associated neuronal abnormalities and neuroAIDS as well.

MATERIALS AND METHODS

Synthesis of Magnetic Nanoparticles

The co-precipitation method was used for synthesis of magnetic nanoparticles.[14] Briefly, Fe^{2+} and Fe^{3+} ions were co-precipitated in alkaline solution and treated under hydrothermal condition. Thoroughly mixed solution of 1 M $FeSO_4 \cdot 7H_2O$ and 2 M $FeCl_3$ were added to 8 M ammonium hydroxide (Sigma) under constant stirring at 25 °C. This results in black magnetite particles. In order to remove impurity such as chloride and sulphate ions, synthesized particles were washed with hot distilled water several times. The purified particles were dispersed in Tris-EDTA buffer (pH 7.5) at a concentration of 10 mg/ml for further use. Quantification of precipitated magnetic nanoparticles was performed by aliquoting and drying particles suspension in an oven at 60 °C to a constant mass.

Transmission Electron Microscopy (TEM) Analysis

TEM of MNPs was performed with the Phillips CM-200 200 kV transmission electron microscope operated at 80 kV.[15] In brief, a drop of MNPs was spread on carbon support film on 400 mesh Cu grids (Type B, Ted Pella, Inc., USA). For better contrast during TEM imaging, samples on grid were negatively stained with phosphotungstic acid (2.0% w/v; pH 6.4) and dried at room temperature.

Zeta Potential

The hydrodynamic radius, size distribution, and surface charge measurement of MNPs were carried out at 25 °C in dynamic laser scattering (DLS) (90 Plus Particles Size Analyzer, Brookhaven Instrument Corp., USA). Samples were prepared by diluting equal quantity of magnetic particles in different pH range of Tris-HCL and Tris-EDTA buffer.

CTOP Binding to Magnetic Nanoparticles: High-Performance Liquid Chromatography/ Photo Diode Array (HPLC/PDA)

Mixture of MNPs and CTOP procured from Sigma Aldrich at different mole ratios (1:0.16, 1:0.33, 1:0.66, 1:1, and 1:1.33) were incubated in tube rotator at room temperature and supernatants were collected for quantification of unbound CTOP by HPLC. The difference between the total CTOP added and unbound CTOP was used to calculate the amount of CTOP bound to the MNPs through HPLC/PDA.

HPLC/PDA analyses were performed with a P4000 Thermo-Finnigan chromatograph (Thermo Electron Corporation, San Jose, California) and consisted of a SpectraSystem SMC1000 solvent delivery system, vacuum membrane degasser, P4000 gradient pumps and AS3000 autosampler. Column effluent was monitored at 254 nm with a SpectraSystem UV6000LP variable wavelength PDA detector and ChromQuest 4.1 software. Analytical separations were carried out with a C18 RP Hypersil GOLD column (RP5, 250 × 4.6 mm, pore size 5 μm, Thermo Electron Corporation). The mobile phase consisted of 0.1% TFA in MeCN (phase A) and 0.1% TFA in H_2O (phase B). The linear gradient program was as follows: 10 to 100% A over 30 min at a flow rate of 1.0 mL/min; 10–20μL of solution were usually injected. Peptide: Rt, 11.30 min; λ_{max} 276 nm.

Fourier Transform Infrared Spectroscopy (FTIR)

FTIR spectroscopy was performed on drug loaded and free nanoparticles to examine the immobilization of CTOP on its surface.[15] Briefly, MNPs bound CTOP isolated from binding reaction mixture were lyophilized to preserve the integrity of drug in the dried and powered MNPs colloids. These powdered samples were used for FTIR analysis in the IR spectrophotometer (Perkin Elmer Spectrum™ 100). Spectra measurements were performed using attenuated total reflection (ATR) on a single bounce diamond/ZnSe ATR crystal. The spectra were collected in the mid-infrared range of 4000–600 cm^{-1} (2.5–25 μm).

Fluorescent Tagging of CTOP for Binding Validation

Alexa flour 610 succinimidyl ester (NHS ester) (Life Technologies) were used for tagging of CTOP. NHS esters were mixed with equal amount of CTOP solution and PBS and were incubated overnight at room temperature. MNPs were added in the mixture and rotated in tube rotator at room temperature. The collected magnetic particle is used for quantification of attached peptide. Fluorescent intensity was measured at wavelength 485/20 nm–528/20 nm (Ex/Em) by microplate reader (Synergy HT, Multi-mode microplate reader, BioTek Instrument, Inc., Winooski, Vermont, USA). MNPs added in mixture of NHS esters and PBS does not show any fluorescent.

Cell Culture

Peripheral blood mononuclear cells (PBMCs), isolated by density gradient centrifugation as described by Gandhi et al.,[16] were cultured in RPMI 1640. RPMI 1640 culture medium was supplemented with 10% fetal bovine serum (FBS), 100 U/ml penicillin, and 100 mg/ml streptomycin (Gibco-BRL, Gaithersburg, MD). Cells were cultured at 37 °C in 5%CO_2 incubator.

SK-N-MCs, a neuroepithelioma cell line derived from a metastatic supra-orbital human brain tumor, were cultured in minimum essential medium (MEM). MEM was supplemented with 10% fetal bovine serum (FBS), 100 U/ml penicillin, and 100 mg/ml streptomycin (Gibco-BRL, Gaithersburg, MD). Cells were incubated at 37 °C in 5%CO_2 incubator. Similarly, primary human brain microvascular endothelial cells (HBMEC) and human astrocyte (HA) cells were cultivated as per provider’s recommendations.

Apoptosis Inhibition Efficiency

Level of apoptosis in each experimental group was analyzed by flocytometry (FACScalibur) using Annexin V: PE Apoptosis detection kit 1 (BD Biosciences) as described by the manufacturers.

Confocal Microscopy and Characterization of Neuro-Spinal Architecture

Membrane staining of neuronal cells for confocal microscopy and measurement of spine density was performed according to the method adopted from Atluri et al.[17,18] The spine density is calculated as the number of spines per unit dendritic length[19] and expressed as spines/μm^2.

HIV Co-Infection of SK-N-MC with Morphine Treatments

0.5 × 106 SK-N-MC cells were seeded onto 22 × 50 mm glass coverslips placed in a 90 mm petri-dish and allowed to adhere overnight. Cells were treated with polybrene (10 μg/ml) and 8 hrs following this treatment, 100 ng clade B HIV-1 was added to each treatment. 12 hr post-infection, non-absorbed virus was washed with PBS, and HIV infection was carried for 7 days. Infected cells were treated with Morphine and CTOP as explained above. Similarly, co-infected cells were DIL stained and prepared for confocal microscopy. The culture supernatant from HIV infected SK-N-MC cells were collected for quantitation of HIV p24 antigen using a p24 ELISA kit (ZeptoMetrix, Buffalo, NY) as described by Atluri et al.[17,18]

Cell Viability Assay

The MTT (Thiazolyl blue tetrazolium bromide) cell proliferation assay was performed as described by Kurapati et al.[20] Briefly, cells from different experimental groups were treated with 0.5% MTT at the rate of 100 μl per well and gently rocked in dark at room temperature for 2–3 hrs. One volume STOP solution containing 20% SDS in 50% dimethyl formamide were added to the rocking cell suspension in MTT solution and further gently rocked in dark at room temperature for 1–2 hrs. Cell suspension is centrifuged at 2000 rpm for 10 minutes and supernatant were collected for the spectrophotometric measurement of optical density of the solubilized formazan at 550 nm. The optical density of formazan in each treatment groups is directly proportional to the cell viability. Cell viability for SK-N-MC were determined similar to that for PBMCs except overnight culture media were changed with 1 ml fresh media before addition of 0.5% MTT.

In Vitro Blood-Brain Barrier (BBB) Model and Transmigration Study

The BBB model was established using HBMEC and HA cells and its intactness was determined by measuring the transendothelial electrical resistance (TEER) using Milli-cell ERS microelectrodes (Millipore) as described earlier by Gandhi et al.[16]

Transmigration study of magnetic nanoparticles was conducted on the 5th-6th day of the BBB culture when ideal integrity of this membrane was achieved as established by TEER measurement. Equal quantity of MNPs were added to the apical chambers and incubated at 37 °C in the presence or absence of a magnetic force placed externally below the trans-well's basal chamber. Samples were collected from both the chambers at different time

points and apparent permeability of MNPs across BBB were calculated by quantifying transmigrated MNPs as described by Hong et al.[14]

RESULTS AND DISCUSSION

Characterization of Magnetic Nanoparticles

Size and topology of MNPs were characterized using TEM (Fig. 1). The average size of magnetic particles is estimated about 25–40 nm. It is known that the higher surface to volume ratio enhances target-affinity of MNPs in comparison to the micro-sized magnetic particles and can even manipulate and target at the subcellular organelles levels. It has also been established that smaller particles (<10 nm) are lost to extravasation and larger particles (>200 nm) are quickly captured and excreted. Particles between 10–70 nm have been shown to penetrate capillary vessels.[21] Thus, synthesized MNPs found to be compatible to enhance drug delivery across the tightly junctioned BMECs along the capillaries lining throughout the cerebral microvasculature. Furthermore, in view of the fact that particles between 70–200 nm possess longer blood circulation time, MNPs of 25–40 nm size could be successfully hybridized with liposomes for synthesis of magnetoliposomes of about 100 nm which will enhance the bioavailability of associated drugs. Importantly, MNPs of around 30 nm size exhibit superparamagnetism and can respond to an external magnetic field. We have shown earlier that magnetic hysteresis loops for these particles, which displayed strong magnetic property, is measured between +1200 and −1200 oersted (Oe).[14] Thus, it would be possible to “remote control” the movement of drug loaded nanoparticles for target-specific delivery by applying the magnetic force at the exterior of desired site.

Effect of pH on Surface Charge Distribution of MNPs

Aqueous solutions of MNPs (Fe_3O_4) perform amphoterism due to adsorption of amphoteric hydroxyl (−OH) group and develop positive or negative charges at the magnetite-water interface in pH-dependent manner.[22] The tunability in the surface charge allow binding of wide range of biomolecule either via direct, but weak, ionic interactions to the MNPs or via surface coating or tethering agents.[23,24] Thus, adsorption efficiency of a molecule on surface of MNPs is influenced by pH of reaction mixture. The magnitude of charge at the surface of colloidal system is quantified by zeta potential. The measurement of zeta potentials at the surface of MNPs in different pH range of Tris-EDTA buffer are shown in Figure 2(A). Our results show that the isoelectric point (*pI*) of MNP is about 7.0 and have positive and negative charge below and above *pI* respectively. We obtained a significant negative zeta potential value (−20.93) at pH 7.4, which is also the physiological pH range. Thus, it is possible that at pH 7.4, MNPs may have sufficient charge for the adsorption of drug molecules. A model for electrostatic interaction between MNPs and CTOP has been illustrated in Figure 2(B). CTOP possess reactive free functional groups such as OH, NH_2, etc. These functional groups may gain charges such as OH^+_2 and NH^+_3 due to change in pH of aqueous media and may influence peptide amphiphilic properties. Therefore, negative charge on the surface of MNPs at pH 7.4 and possible positive charges moieties in the drugs may allow direct binding via ionic interaction. Alternatively, MNPs-CTOP binding due to chelating or hydrophobic interactions cannot be denied. The binding of molecules to MNPs

can be reversible due to pH variation, which may allow the bound drugs to be released at the target site.

CTOP Adsorption on MNPs Surface

FTIR spectra identifies the bending vibration of surface bonding of functional groups present on a compound.[25] It creates compound-specific molecular fingerprint in the form of absorption and/or transmission spectrum. Two state of same molecule have different bending vibration of its functional groups resulting in different pattern of FTIR spectra. As such, FTIR spectroscopy was performed to the lyophilized MNPs bound with or without CTOP. Typically, bending vibration at about 900–1000 cm^{-1} corresponds to the O–H bond, particularly for strong hydrogen bridges. Similarly, about 1000–1600 cm^{-1} is typical of the H–O–H molecule.[26] In order to define the presence of CTOP on MNPs, transmittance spectra of "MNPs-CTOP" were subtracted from that of MNPs only and percent transmittance difference were plotted (Figs. 3(A) and (B)). Maximum variation in transmittance was detected at about 600–1600 cm^{-1}. We can see a reduction in transmittance up to 18% at 1025 cm^{-1} for CTOP bound MNPs. Thus, change transmittance for "MNP + CTOP" in compare to MNPs at these bands may correspond to two interrelated phenomenon. First, hydroxyl groups from water molecule may have attached by the hydrogen bonds in the Fe_3O_4 surface influencing the negative charge distribution on surface which is reflected as higher negative zeta potential. Similarly, water molecules (H–O–H) may have chemically adsorbed to the magnetic particle surfaces, again influencing the surface charge ($Fe–OH + H^+ = Fe–OH_2/Fe–OH = Fe–O^- + H^+$). Second and more importantly, presence of charge due to O–H or H–O–H on the surface of MNPs might have allowed binding of CTOP resulting in change of bending vibration of bonds which may be reason of reduced transmittance. Additionally, we noticed that transmittance of "MNP + CTOP" is also reduced up to 7% at about 2870 cm^{-1} and 3370 cm^{-1} which may reflect increased absorption at these bands due to presence of additional CH and NH_2 group of CTOP. Typically, frequency range for N–H group is 3300–3500 cm^{-1} and that of C–H is 2700–3300 cm^{-1}. CTOP absorption on the surface of MNPs was further verified using fluorescent-based detection method. The Alexa flour 610 succinimidyl (NHS) esters were used for tagging of this peptide (data not shown). The NHS ester mediated bonding is most efficient and convenient way to attach fluorophores to amine-containing ($R\text{-}NH_2$) molecules such as peptides, proteins, or amine-modified nucleic acids. The stability of amide bonds formed in the reaction is as good as that of peptide bonds. Thus, selective linking of fluorophores to peptides opens window for many purposes such as quantification, imaging, etc. Significant fluorescent intensity was detected on the MNPs immobilized with dye tagged peptide. Simultaneously, dye-exposed or non-exposed MNPs showed no trace of fluorescent activity. This suggests that CTOP could successfully be immobilized on the surface of MNPs.

Time Kinetics and Binding Isotherm of CTOP to MNPs

Data presented in the Figures 4(A) and (B) shows the time kinetics and percent direct binding of CTOP to MNPs, respectively. We found a significant binding of CTOP to magnetic nanoparticles. The MNPs were dispersed in Tris-EDTA buffer (pH 7.4) and mixed with CTOP. The mixture was incubated in tube rotator at room temperature and supernatant

were collected at different time points from 5–240 minutes (Fig. 4(A)). The unbound fraction of CTOP present in supernatant was quantified by HPLC. The difference between the total CTOP added and unbound CTOP was used to calculate the amount of CTOP bound to the MNPs. Maximum binding was achieved at about 5 minutes of incubation which remained unaffected till 4 hour of experimental duration. After the time kinetics of binding was optimized, the CTOP binding efficiency was estimated by using different ratios (Weight/Concentration), 1:0.16, 1:0.33, 1:0.66, 1:1, and 1:1.33 of MNPs and CTOP, respectively. Data presented in Figure 4(B) show the adsorption isotherm of CTOP on MNPs. The result obtained from three independent experiments indicates a maximum binding efficiency of about 140 μg CTOP per mg of MNPs. It should be noted that time kinetics and loading efficiency significantly affect the drugs sustainability and safe dosing. This eventually influences drugs bioavailability. The sustainable binding of CTOP on MNPs for over four hours is in accordance to our hypothesis where, under the non-invasive magnetic influence, drug delivery to the target could be maximized before it leaches out of the nanocarrier.

Functional Efficiency of MNPs Bound CTOP

Inhibition of Morphine-Induced Peripheral Pathogenesis—Exposure of drug abuse including morphine has been shown to modulate functions of various immune cells such as phagocytes, *T* cells, dendritic cells, etc.[27–32] It significantly alters the expression of cytokines, chemokines, etc. and induces apoptosis in both peripheral and neuronal cells. Studies from our lab[33] have shown that morphine exposure causes significant induction of apoptosis in PBMCs. Though different kinds of opioid receptors exist, morphine exerts its effect primarily through the μ opioid receptor. Therefore, use of a μ opioid receptor antagonist could prevent the morphine-induced effect and may provide significant therapeutic benefits. We used D-Pen-Cys-Tyr-DTrp-Orn-Thr-Pen-Thr-NH_2 (CTOP), which is a highly selective and potent μ receptor antagonist and remains impenetrable through the brain barriers. To compare the efficiency of MNPs bound CTOP with that of free CTOP, PBMCs were treated with morphine and its effect on apoptosis induction was analyzed using flow-cytometry (Fig. 5). Annexin-V is the indicator protein of the earliest events in apoptosis. As expected, more than 80% of PBMCs were found to be Annexin-V positive when they were treated with morphine (Figs. 5(C) and (F)). This effect was significantly reversed when cells were treated with free or MNPs bound CTOP (Figs. 5(D)–(F)). Number of Annexin-V positive cells was reduced approximately by 50% upon treatment with free CTOP and only 32% cells were found Annexin-V positive. Similarly, MNPs-bound CTOP exerted equivalent apoptosis inhibition efficiency and nearly 24% cells were found Annexin-V positive in this case. Untreated or only MNPs treated cells showed near zero or insignificant induction of apoptosis. Thus, our result suggests that efficacy of CTOP upon its binding to MNPs is preserved.

Inhibition of Morphine-Induced Neuronal Pathogenesis

Studies have shown that drug addiction alters the function of the neuronal circuit which includes changes in neuronal plasticity and synaptic transmitter release.[34–36] Similarly, morphine administration produces a persistent decrease in dendrite length and dendritic spine in neurons of different brain regions such as nucleus accumbens, visual cortex, sensory

cortex, etc.[37,38] Morphine crosses the brain barriers and believed to suppress CNS immune responses by various mechanisms. It inhibits or downregulates various inflammation-suppressing chemokines and cytokines such as macrophage inflammatory protein, interleukin-8 etc.[39] Also, morphine has been shown to induce apoptosis in various CNS cells such as microglia, astrocytes, neurons, etc.[40–42] All these immune-inhibitory effect of morphine could influence neuro-inflammation leading to neuropathogenesis. In fact, deregulation of chemokine or cytokine expression in CNS cells is a hallmark phenomenon associated with neuronal degeneration. As such, morphine is putatively believed to acts synergistically as a co-factor in neuropathogenesis. In particular, morphine has been shown to synergize the HIV infection associated neurocognitive disorders where spinal architecture of neuronal cells is significantly altered.[17] Figure 6(B) and (C) shows altered spinal morphology of neurob-lastoma cells upon morphine treatment. This alteration of spinal architecture may negatively affect the synaptic plasticity during morphine exposure. Spine morphology play important role in maximizing the effectiveness of the synaptic transmission leading to cognitive modulation. Neuronal adaptation pattern is differentially regulated during opioid addiction[43] and cause rapid development of tolerance, physical and psychological dependence. These opioid-dependence associated disorders could significantly be diminished by supplementation of anti-opioid agents which may prevent opioid-induced pathogenesis. However, current treatments to alleviate the action of opioids are less effective at CNS level, basically due to impermeability of therapeutic molecules across brain barriers. As a first step towards our hypothesis in developing MNPs-based nanoformulations of anti-opioid agents, we analyzed the efficiency of MNPs bound CTOP in preventing the morphine induced inhibition of spinal density as a sign of neuronal degeneration (Fig. 6). As shown in Figure 7, morphine treated cells showed a spinal density of 0.24 ± 0.07 per μm^2, whereas the same in untreated cells were approximately 1 per μm^2 ($P < 0.0001$). This significant decrease in morphine-induced spinal density is prevented upon CTOP treatment. Both free and MNPs-bound CTOP showed equivalent efficiency in checking the spinal degeneration (Figs. 7; 6(E) and (F)). Cells with free CTOP and MNPs bound CTOP showed an average spine density of 1.04 ±0.18 and 0.84 ±0.30 per μm^2 respectively.

These values were comparable to that of untreated cells; however were significantly higher than that of morphine treated cells only ($P < 0.0001$). Treatment of MNPs alone in cells exposed or non-exposed to morphine (Figs.7; 6(C) and (B)). did not alter the spinal density. Thus, our result suggests that, similar to their efficacy in suppressing apoptosis induction in PBMCs, MNPs bound CTOP possesses parallel effect to that of free CTOP in preserving the neuropathogenesis.

Inhibition of Morphine-Induced Neuronal Pathogenesis During HIV Infection

As discussed previously, opioids act in synergy with HIV viral proteins and cause greater immunosuppression. Regions of brain with higher opioid receptors such as striatum and hippocampus have been shown to possess increased viral titers[5,44,45] which lead to faster neuropathogenesis. As such, we analyzed the efficiency of MNPs-bound CTOP in preventing the additive neuro-degeneration of morphine during HIV infection. As reported previously from our laboratory,[17] HIV infections lead to severe loss of spinal architecture in

neuroblastoma cells (Fig. 8(B)). In comparison with uninfected cells where spinal density was approximately 1 per μm^2, HIV infections reduce the spinal density to 0.35 ±0.17 per μm^2 ($P < 0.0001$) and, though not significant, it goes further down to 0.30 ±072 per μm^2 when exposed to morphine during infection (Figs. 8(B) and (C); 9). To analyze the efficacy of our MNP-CTOP nanoformulation in prevention of morphine-induced additive neuropathogenesis, morphine-exposed-HIV-infected cells were treated with MNPs bound CTOP. As shown in Figures 8(D) and 9, this significantly prevented the spinal degeneration. The spinal density significantly went up to 0.74 ±078 per μm^2 compared to HIV infection ($P < 0.0002$) or co-treatment of morphine with infection ($P < 0.0001$) (Fig. 9). Upregulation of μ opioid receptor and associated alteration in the expression of pro- and antiapoptotic molecules, cytokines, and chemokines are common phenomena during the HIV infection and opioid exposure.[8,45–49] Apoptosis due to treatment with HIV-1 pathogenic protein gp120 and morphine in μ-opioid receptors deficient mice gets lowered significantly in comparison with the wild types.[50] The magnetic nanoformulations carrying μ-opioid receptor antagonist, CTOP, could possibly block this receptor and, thus, in turn, may minimize the neuro-pathogenesis exacerbated due to morphine co-treatment and/or HIV infection. Therefore, as our result suggests (Figs. 6–9), higher spinal density in HIV infected and morphine co-treated neuronal cells, upon exposure of MNP bound CTOP, should be a natural outcome than cells where no CTOP was supplied. This further, supports our hypothesis in developing MNPs-based nanoformulations of anti-opioid agents.

Cytotoxicity of MNPs-Bound CTOP

One of the major concerns while using nanomaterials in medicine is that of potential toxicity. Any exposure of external insults in the body, particularly when a sensitive organ such as brain is targeted, must be validated for its cytotoxic effect. As such, evaluation of cell viability is important for the nanoparticle application in medicine. It has been suggested that doses of MNPs within the permissible limit have non-significant safety concerns and are biodegradable.[51] We examined the nonspecific cytotoxicity of MNPs with and without CTOP to PBMCs and SK-N-MCs. Our results showed that MNPs were neither cytotoxic to PBMCs nor to SK-N-MCs up to 48 hours of experimental treatments (data not shown). The unaffected percent cell viability due to treatments of MNP with or without CTOP compared to untreated cells indicates their safe use as nanocarrier for drug deliver.

BBB Transmigration Ability of the MNPs

In a proof-of-concept experiment, magnetic force-driven delivery of MNPs across BBB was performed in the endothelial cells–astrocytes co-culture *in vitro* BBB model (Fig. 10). In this most widely accepted BBB model, endothelial cells and astrocytes are respectively grown to confluency on top and underside of porous membrane of a transwell. The transwell bicompartmentalizes the culture plate such that the top and underside of porous membrane with cells mimics the external (peripheral blood side) and internal (brain microenvironment side) face of BBB, respectively. The transmigration efficacy of MNPs was measured by its permeability from upper chamber to lower chamber under influence of external magnetic force. Quantification of iron concentration in the lower chamber shows that application of external magnetic force for 1 and 2 hr resulted in 2.2 and 2.7 fold higher MNPs transmigration, respectively (Fig. 10(B)). A larger MNPs permeability may be possible with

increased duration of magnetic force. The TEER values of grown BBB before and after MNPs treatment were found to be near 200 Ω/cm^2 (Fig. 10(C)). These TEER values are consistent with the formation of near natural-intact BBB suggesting MNPs do not affect the BBB integrity. Significantly higher trans-endothelial migration of MNPs as early as 1–2 hours of experimental period suggest that a MNP-based drug nanocarrier may speedily transport associated drugs to the brain under magnetic influence. As such, it may effectively reduce the peripheral circulatory time and RES exposure. Nevertheless, dugs bound naked nanoparticles may be decomposed due to metabolic (enzymztic mainly) activity of peripheral circulation (blood) before it reaches to the brain. So, eencapsulation of MNPs bound drugs within the core of liposomes (magnetized liposomes) could be a very promising material for clinical applications because it can remarkably improves the drug stability and bioavailability in blood circulation. Magnetized liposomes can also be transported across BBB under influence of external magnetic force. Additionally, per unit loading efficiency of the hybridized magnetic liposomes could be improved by supplementing free dugs on its phospholipid bilayers around its MNPs filled core. As such we propose a novel “magneto-liposome” nanocarrier which can reduce the drug decomposition, clearance, and entrapment from the naked MNPs in the peripheral (blood) circulation.

CONCLUSION

In the wake of the fact that almost all small or large therapeutical drugs are unable to cross the BBB—which is believed to be main impediment in cure of neurological disorders—several strategies are being experimented to administer the desired therapeutic levels of drugs in brain. In an effective drug delivery method, majority of therapeutic agents should be delivered to the target site while non-target site should get minimal drug exposure. Complying with this notion, practice of nanotechnology in medicine has shown exciting prospect for development of novel targeted delivery system.[52–56] MNPs possess distinct advantage for its use as a platform for theranostic nanomedicine for CNS diseases because it could simultaneously be used as carrier for speedy and targeted drug delivery (mediated by external non-invasive magnetic force) and MRI contrast agent (due to inherent superparamagnetism). In our studies, as a first step towards specific drug targeting to prevent the neuropathogenesis associated with recreational drugs, we have developed for the first time a MNPs based nanoformulation, which shows that CTOP (a μ opioid receptor blocker : anti-opioid agent) can be immobilized on MNPs. Our studies indicate that MNPs-CTOP nanoformulation effectively suppress the morphine induced pathological conditions in peripheral and neuronal cells. More importantly, the developed nanoformulation could significantly prevent the morphine induced neuropathogenesis in HIV-1 *in vitro* infection model. Further as a proof-of-concept we found that MNPs can transmigrate across BBB under the influence of external, non-invasive magnetic force. Therefore, the delivery of CTOP and other anti-addiction drugs using MNPs is expected to be of more therapeutical benefit and, in turn, may reduce the risk of developing recreational drugs associated neuropathogenesis and neuroAIDS.

Acknowledgment

This work was supported in part by grants R01DA027049, R37DA025576, and 1R21MH101025 from the National institute on Drug Abuse. We also would like to appreciate the assistance of Dr. Yong Cai (Department of Chemistry and Biochemistry, Florida International University) and late Horacio Priestap (Department of Biological Sciences, Florida International University) in DLS measurement and HPLC analysis, respectively.

REFERENCES

1. UNODC. World Drug Report (United Nations publication, Sales No. E.12.XI.1). 2012
2. Hauser KF, El-Hage N, Stiene-Martin A, Maragos WF, Nath A, Persidsky Y, Volsky DJ, Knapp PE. HIV-1 neuropathogenesis: Glial mechanisms revealed through substance abuse. J. Neurochem. 2007; 100:567. [PubMed: 17173547]
3. Ferris MJ, Mactutus CF, Booze RM. Neurotoxic profiles of HIV, psychostimulant drugs of abuse, and their concerted effect on the brain: Current status of dopamine system vulnerability in NeuroAIDS. Neuroscience and Biobehavioral Reviews. 2008; 32:883. [PubMed: 18430470]
4. Rogers TJ, Immunology as it pertains to drugs of abuse. AIDS and the neuroimmune axis: Mediators and traffic. Journal of Neuroimmune Pharmacology. 2011; 6:20. [PubMed: 20957520]
5. Hauser KF, El-Hage N, Buch S, Berger JR, Tyor WR, Nath A, Bruce-Keller AJ, Knapp PE. Molecular targets of opiate drug abuse in neuro AIDS. Neurotoxicity Research. 2005; 8:63. [PubMed: 16260386]
6. Reddy PVB, Pilakka-Kanthikeel S, Saxena SK, Saiyed Z, Nair MP. Interactive effects of morphine on HIV infection: Role in HIV-associated neurocognitive disorder. AIDS Research and Treatment. 2012:2012.
7. Peterson PK, Molitor TW, Chao CC. The opioid–cytokine connection. Journal of Neuroimmunology. 1998; 83:63. [PubMed: 9610674]
8. El-Hage N, Gurwell JA, Singh IN, Knapp PE, Nath A, Hauser KF. Synergistic increases in intracellular Ca^{2+}, and the release of MCP-1, RANTES, and IL-6 by astrocytes treated with opiates and HIV-1 Tat. Glia. 2005; 50:91. [PubMed: 15630704]
9. Stefano GB, Scharrer B, Smith EM, Hughes TK Jr, Magazine HI, Bilfinger TV, Hartman AR, Fricchione GL, Liu Y, Makman MH. Opioid and opiate immunoregulatory processes. Critical Reviews™ in Immunology. 1996; 16
10. Sagar V, Pilakka-Kanthikeel S, Pottathil R, Saxena SK, Nair M. Towards nanomedicines for neuroAIDS. Reviews in Medical Virology. 2014
11. Sagar V, Pilakka-Kanthikeel S, Ding H, Atluri VSR, Jayant RD, Kaushik A, Nair MP. Novel magneto-electric nanode-livery of microRNA mimic across blood-brain barrier: Implicationsy to cocaine modulation on HIV-associated neurocognitive disorders. Journal of NeuroImmune Pharmacology. 2014; 9:49.
12. Kaushik A, Jayant RD, Sagar V, Nair M. The potential of magneto-electric nanoparticles for drug delivery. Expert Opinion on Drug Delivery. 2014; 11:1635. [PubMed: 24986772]
13. Pilakka-Kanthikeel S, Atluri VSR, Sagar V, Nair M. Targeted brain derived neurotropic factors (BDNF) delivery across the blood-brain barrier for neuro-protection using magnetic nano carriers: An *in-vitro* study. Plos One. 2013; 8:e62241. [PubMed: 23653680]
14. Ding H, Sagar V, Agudelo M, Pilakka-Kanthikeel S, Atluri VSR, Raymond A, Samikkannu T, Nair MP. Enhanced blood–brain barrier transmigration using a novel transferrin embedded fluorescent magneto-liposome nanoformulation. Nanotechnology. 2014; 25:055101. [PubMed: 24406534]
15. Nair M, Guduru R, Liang P, Hong J, Sagar V, Khizroev S. Externally controlled on-demand release of anti-HIV drug using magneto-electric nanoparticles as carriers. Nature communications. 2013; 4:1707.
16. Gandhi N, Saiyed ZM, Napuri J, Samikkannu T, Reddy PV, Agudelo M, Khatavkar P, Saxena SK, Nair MP. Interactive role of human immunodeficiency virus type 1 (HIV-1) clade-specific Tat protein and cocaine in blood-brain barrier dysfunction: implications for HIV-1-associated neurocognitive disorder. Journal of Neurovirology. 2010; 16:294. [PubMed: 20624003]

17. Atluri VSR, Kanthikeel SP, Reddy PV, Yndart A, Nair MP. Human synaptic plasticity gene expression profile and dendritic spine density changes in HIV-infected human CNS cells: Role in HIV-associated neurocognitive disorders (HAND). Plos One. 2013; 8:e61399. [PubMed: 23620748]
18. Atluri VSR, Pilakka-Kanthikeel S, Thangavel S, Sagar V, Rao KVK, Saxena SK, Yndart A, Raymond A, Ding H, Hernandez O, Nair M. Vorinostat positively regulates synaptic plasticity genes expression and spine density in HIV infected neurons: Role of nicotine in progression of HIV-associated neurocognitive disorder. Molecular Brain. 2014; 7:37. [PubMed: 24886748]
19. Smith DL, Pozueta J, Gong B, Arancio O, Shelanski M. Reversal of long-term dendritic spine alterations in Alzheimer disease models. Proc. Natl. Acad. Sci. U S A. 2009; 106:16877. [PubMed: 19805389]
20. Kurapati KRV, Atluri VSR, Samikkannu T, Nair MP. Ashwagandha (Withania somnifera) reverses β-amyloid1-42 induced toxicity in human neuronal cells: Implications in HIV-associated neurocognitive disorders (HAND). Plos One. 2013; 8:e77624. [PubMed: 24147038]
21. Liu C. Research and application of targeting nano-drugs. Nano Biomedicine and Engineering. 2011; 3:73.
22. Tombacz E, Majzik A, Horvat Z, Illes E. Magnetite in aqueous medium: Coating its surface and surface coated with it. Romanian Reports in Physics. 2006; 58:281.
23. Yoo J-W. Toward improved selectivity of targeted delivery: The potential of magnetic nanoparticles. Arch. Pharmacal Res. 2012; 35:1.
24. iogo HT, Lim M, Bulmus V, Utirre LA, Oodward RC, Amal R. Insight into serum protein interactions with functional-ized magnetic nanoparticles in biological media. Langmuir. 2012; 28:4346. [PubMed: 22313424]
25. Balaji N, Begum KMS, Anantharaman N, Uddin M. Adsorption and desorption of L-Phenylalanine on nano-sized magnetic particles. Journal of Engineering and Applied Sciences. 2006; 4:39.
26. Lopez JA, González F, Bonilla FA, Zambrano G, Gómez ME. Synthesis and characterization of Fe_3O_4 magnetic nanofluid. Revista Latinoamericana de Metalurgia y Materiales. 2010; 60
27. Eisenstein TK, Hilburger ME. Opioid modulation of immune responses: effects on phagocyte and lymphoid cell populations. Journal of Neuroimmunology. 1998; 83:36. [PubMed: 9610671]
28. Messmer D, Hatsukari I, Hitosugi N, Schmidt-Wolf IG, Singhal PC. Morphine reciprocally regulates IL-10 and IL-12 production by monocyte-derived human dendritic cells and enhances T cell activation. Molecular Medicine. 2006; 12:284. [PubMed: 17380193]
29. Rivera-Amill V, Silverstein PS, Noel RJ Jr, Kumar S, Kumar A. Morphine and rapid disease progression in nonhuman primate model of AIDS: Inverse correlation between disease progression and virus evolution. Journal of Neuroimmune Pharmacology. 2010; 5:122. [PubMed: 20013315]
30. Saurer TB, Carrigan KA, Ijames SG, Lysle DT. Suppression of natural killer cell activity by morphine is mediated by the nucleus accumbens shell. Journal of Neuroimmunology. 2006; 173:3. [PubMed: 16364456]
31. Wang J, Barke RA, Ma J, Charboneau R, Roy S. Opiate abuse, innate immunity, and bacterial infectious diseases. Archivum Immunologiae et Therapiae Experimentalis. 2008; 56:299. [PubMed: 18836861]
32. Thangavel S, Rao KVK, Arias AY, Kalaiche ian A, Sagar V, Yoo C, Nair MPN. HIV Infection and drugs of abuse: Role of acute phase proteins. Journal of Neuroinflammation. 2013; 10:113. [PubMed: 24044608]
33. Nair M, Pottathil R, Heimer E, Schwartz S. Immunoregulatory activities of human immunodeficiency virus (HIV) proteins: Effect of HIV recombinant and synthetic peptides on immunoglobulin synthesis and proliferative responses by normal lymphocytes. Proceedings of the National Academy of Sciences. 1988; 85:6498–6502.
34. Sarti F, Borgland SL, Kharazia VN, Bonci A. Acute cocaine exposure alters spine density and long-term potentiation in the ventral tegmental area. European Journal of Neuroscience. 2007; 26:749. [PubMed: 17686047]
35. Frankfurt M, Salas-Ramirez K, Friedman E, Luine V. Cocaine alters dendritic spine density in cortical and subcortical brain regions of the postpartum and virgin female rat. Synapse. 2011; 65:955. [PubMed: 21480383]

36. Nestler EJ. Molecular basis of long-term plasticity underlying addiction. Nazure Reviews Neuroscience. 2001; 2:119. [PubMed: 11252991]
37. Li Y, Wang H, Niu L, Zhou Y. Chronic morphine exposure alters the dendritic morphology of pyramidal neurons in visual cortex of rats. Neuroscience Letters. 2007; 418:227. [PubMed: 17466454]
38. Robinson TE, Kolb B. Alterations in the morphology of dendrites and dendritic spines in the nucleus accumbens and prefrontal cortex following repeated treatment with amphetamine or cocaine. European Journal of Neuroscience. 1999; 11:1598. [PubMed: 10215912]
39. Mahajan SD, Schwartz SA, Shanahan TC, Chawda RP, Nair MP. Morphine regulates gene expression of α-and β-chemokines and their receptors on astroglial cells via the opioid μ receptor. The Journal of Immunology. 2002; 169:3589. [PubMed: 12244149]
40. Goswami R, Dawson SA, Dawson G. Cyclic AMP protects against staurosporine and wortmannin-induced apoptosis and opioid-enhanced apoptosis in both embryonic and immortalized (F-11κ7) neurons. J. Neurochem. 1998; 70:1376. [PubMed: 9523553]
41. Yin D, Mufson RA, Wang R, Shi Y. Fas-mediated cell death promoted by opioids. Nature. 1999; 397:218. [PubMed: 9930695]
42. Hu S, Sheng WS, Lokensgard JR, Peterson PK. Morphine potentiates HIV-1 gp120–induced neuronal apoptosis. Journal of Infectious Diseases. 2005; 191:886. [PubMed: 15717263]
43. Simonato ML. The neurochemistry of morphine addiction in the neocortex. Trends in Pharmacological Sciences. 1996; 17:410. [PubMed: 8990957]
44. Nath A, Anderson C, Jones M, Maragos W, Booze R, Mactutus C, Bell J, Hauser KF, Mattson M. Neurotoxicity and dysfunction of dopaminergic systems associated with AIDS dementia. Journal of Psychopharmacology. 2000; 14:222. [PubMed: 11106300]
45. Nath A, Hauser KF, Wojna V, Booze RM, Maragos W, Prendergast M, Cass W, Turchan JT. Molecular basis for interactions of HIV and drugs of abuse. Journal of Acquired Immune Deficiency Syndromes (1999). 2002; 31:S62–S69. [PubMed: 12394784]
46. Peterson PK, Gekker G, Hu S, Anderson WR, Kravitz F, Portoghese PS, Balfour HH Jr, Chao CC. Morphine amplifies HIV-1 expression in chronically infected promonocytes cocultured with human brain cells. Journal of Neuroimmunology. 1994; 50:167. [PubMed: 8120138]
47. Rojavin M, Szabo I, Bussiere JL, Rogers TJ, Adler MW, Eisenstein TK. Morphine treatment *in vitro* or *in vivo* decreases phagocytic functions of murine macrophages. Life Sci. 1993; 53:997. [PubMed: 8361330]
48. Zhang N, Oppenheim JJ. Crosstalk between chemokines and neuronal receptors bridges immune and nervous systems. Journal of Leukocyte Biology. 2005; 78:1210. [PubMed: 16204635]
49. Beltran JA, Pallur A, Chang SL. HIV-1 gp120 up-regulation of the mu opioid receptor in TPA-differentiated HL-60 cells. International Immunopharmacology. 2006; 6:1459. [PubMed: 16846840]
50. Moorman J, Zhang Y, Liu B, LeSage G, Chen Y, Stuart C, Prayther D, Yin D, HIV-1 gp120 primes lymphocytes for opioid-induced. β-arrestin 2-dependent apoptosis. Biochimica et Biophysica Acta (BBA)-Molecular Cell Research. 2009; 1793:1366. [PubMed: 19477204]
51. Jain TK, Reddy MK, Morales MA, Leslie-Pelecky DL, Labhasetwar V. Biodistribution, clearance, and biocompatibility of iron oxide magnetic nanoparticles in rats. Molecular Pharmaceutics. 2008; 5:316. [PubMed: 18217714]
52. Choi S, Tripathi A, Singh D. Smart nanomaterials for biomedics. J. Biomed. Nanotechnol. 2014; 10:3162. [PubMed: 25992434]
53. Pekkanen AM, DeWitt MR, Rylander MN. Nanoparticle enhanced optical imaging and phototherapy of cancer. J. Biomed. Nanotechnol. 2014; 10:1677. [PubMed: 25992437]
54. Zhang L, Zhao D. Applications of nanoparticles for brain cancer imaging and therapy. J. Biomed. Nanotechnol. 2014; 10:1677. [PubMed: 25992437]
55. Jayant RD, Srivastava R. Dexamethasone release from uniform sized nanoengineered alginate microspheres. Journal of Biomedical Nanotechnology. 2007; 3:1.
56. Ahsan A, Aziz A, Arshad MA, Ali O, Nauman M, Ahmad NM, Elaissari A. Smart magnetically engineering colloids and biothin films for diagnostics applications. J. Colloid Sci. Biotechnol. 2013; 2:19.

57. Roveimiab Z, Mahdavian AR, Biazar E, Heidari KS. Preparation of magnetic chitosan nanocomposite particles and their susceptibility for cellular separation applications. J. Colloid Sci. Biotechnol. 2012; 1:82.

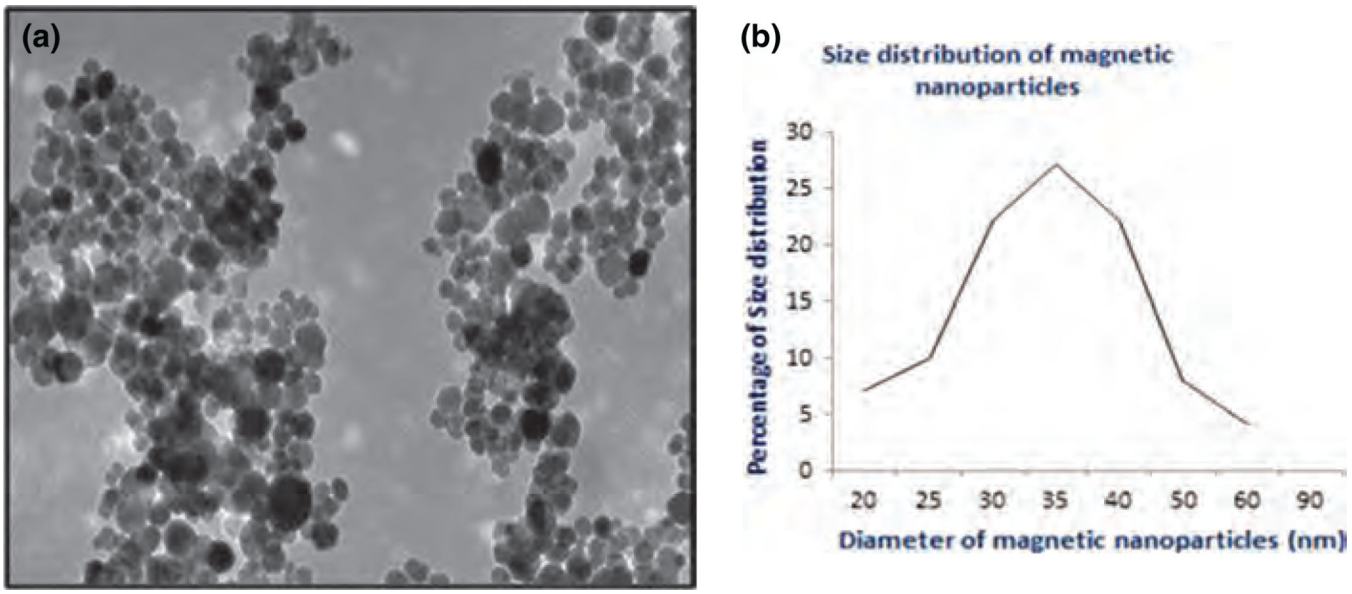

Figure 1.

Characterization of MNPs: (A) Transmission electron micrograph of Fe_3O_4 magnetic particles. (B) Size distribution of magnetic nanoparticles: Average size of nanoparticles is 25–40 nm.

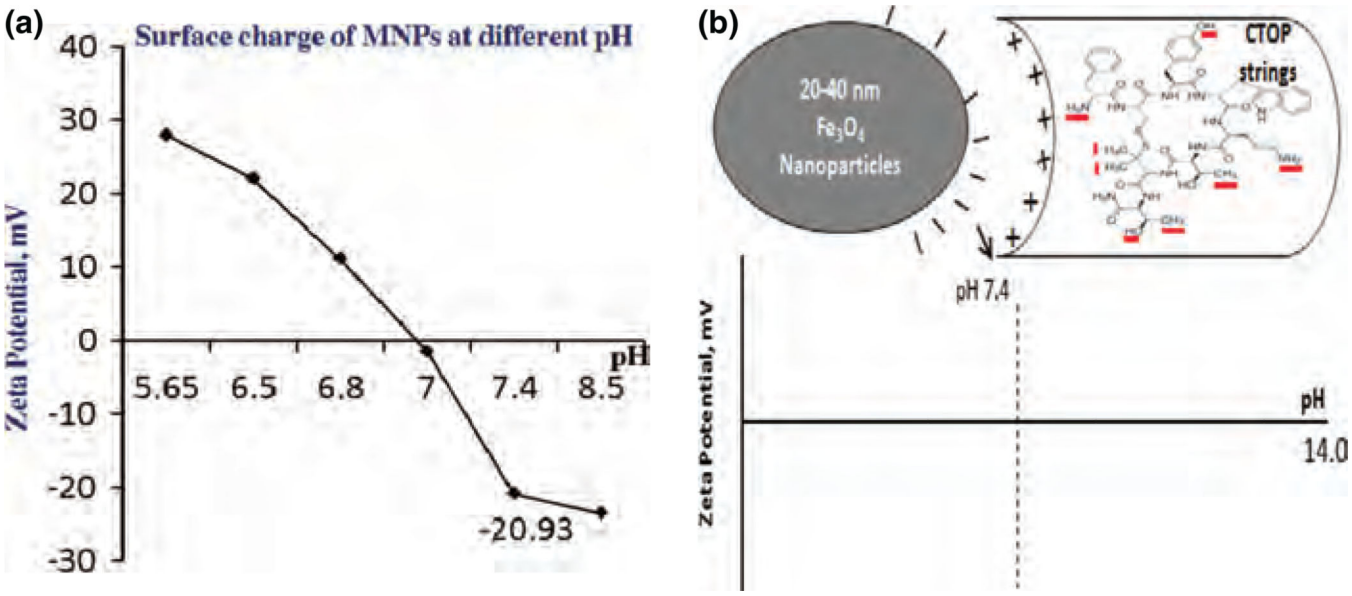

Figure 2.

MNPs surface charge and schematic of MNPs-drug interaction (A) Zeta potential of MNPs at different pH shows that the physiological pH 7.4 generates significant negative charges on its surface. (B) Schematic illustration showing interaction between negative charge on MNPs surface and positive charge on selected moieties (NH_2, CH_3, etc.) of CTOP peptide at pH 7.4.

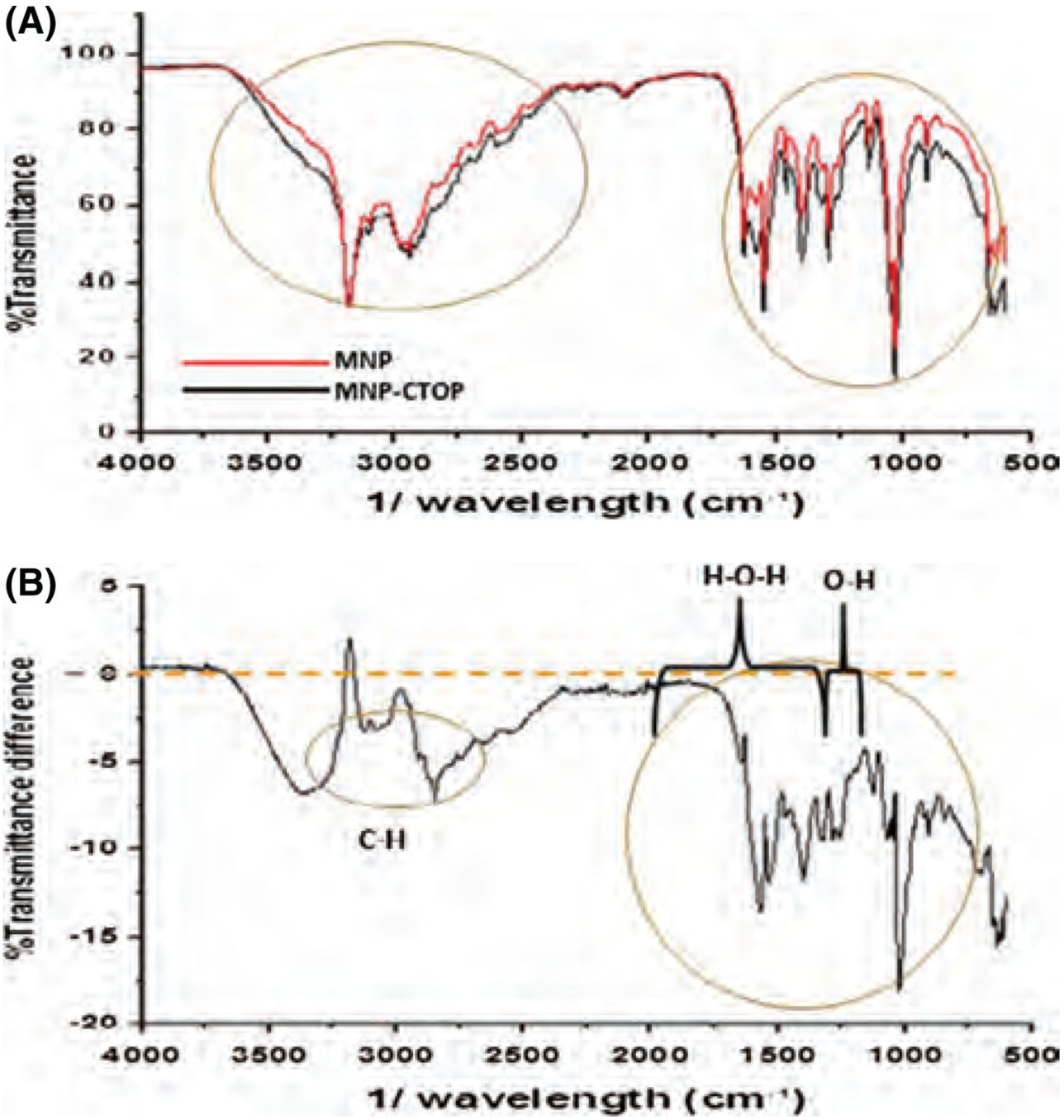

Figure 3.

FTIR spectra of transmittance: (A) % transmittance of MNP and “MNP + CTOP.” (B) Difference between % transmittance of MNP and “MNP+CTOP”: transmittance of “MNP+ CTOP” obtained from FTIR were subtracted from transmittance of MNP and difference in transmittance at specific band ranges were co-related with presence or absence of functional group associated with CTOP and aqueous medium.

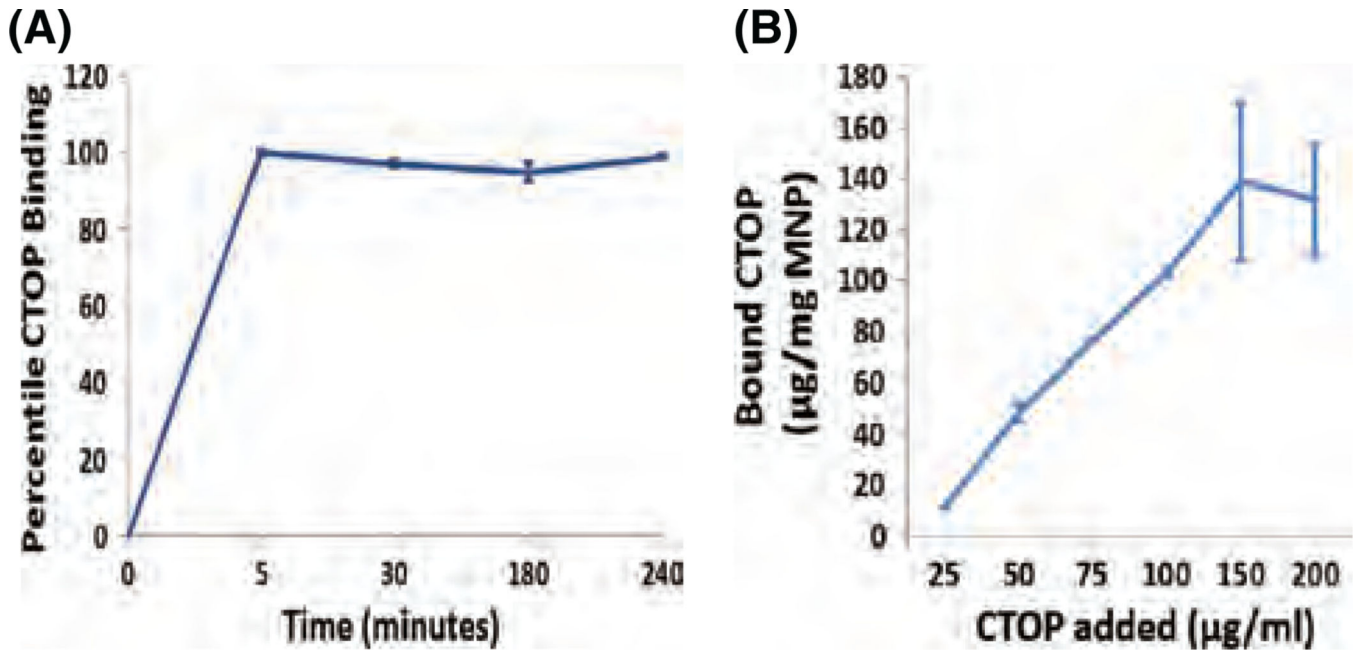

Figure 4.

MNSs-CTOP binding: (A) Time kinetics shows maximum CTOP binding on MNPs is achieved in 5 minutes of reaction time which remains unaffected until 4 hrs of experimental time. (B) Binding isotherm shows maximum binding efficiency of ∼140 µg CTOP on 1 mg MNPs.

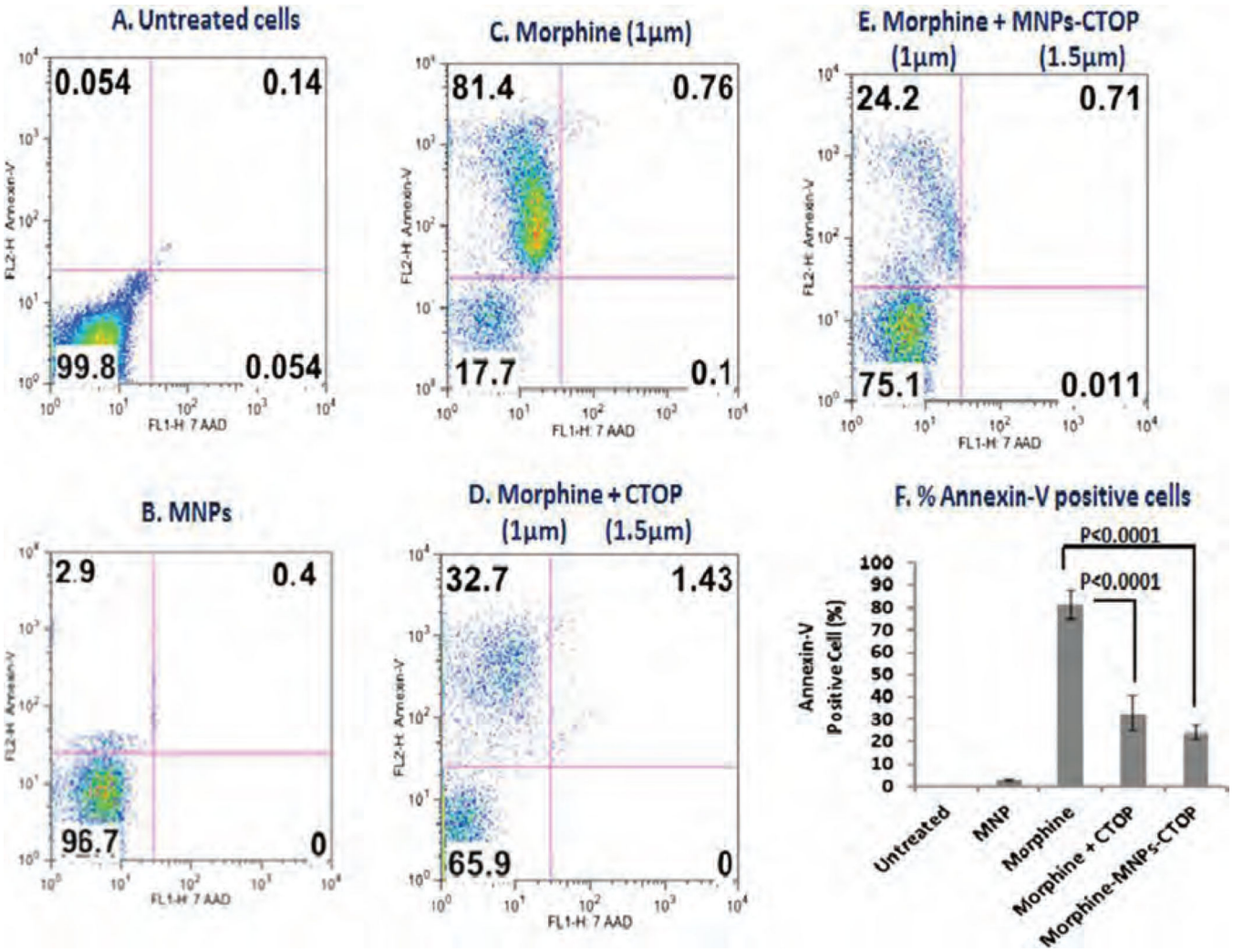

Figure 5.

Flow-cytometry to evaluate the efficacy of MNPs bound CTOP on inhibition of morphine induced apoptosis in PBMCs: % of Annexin-V positive cells shows that MNP bound CTOP (E) possess parallel efficacy to that of free CTOP (D) in suppressing the apoptosis induced by morphine (C).

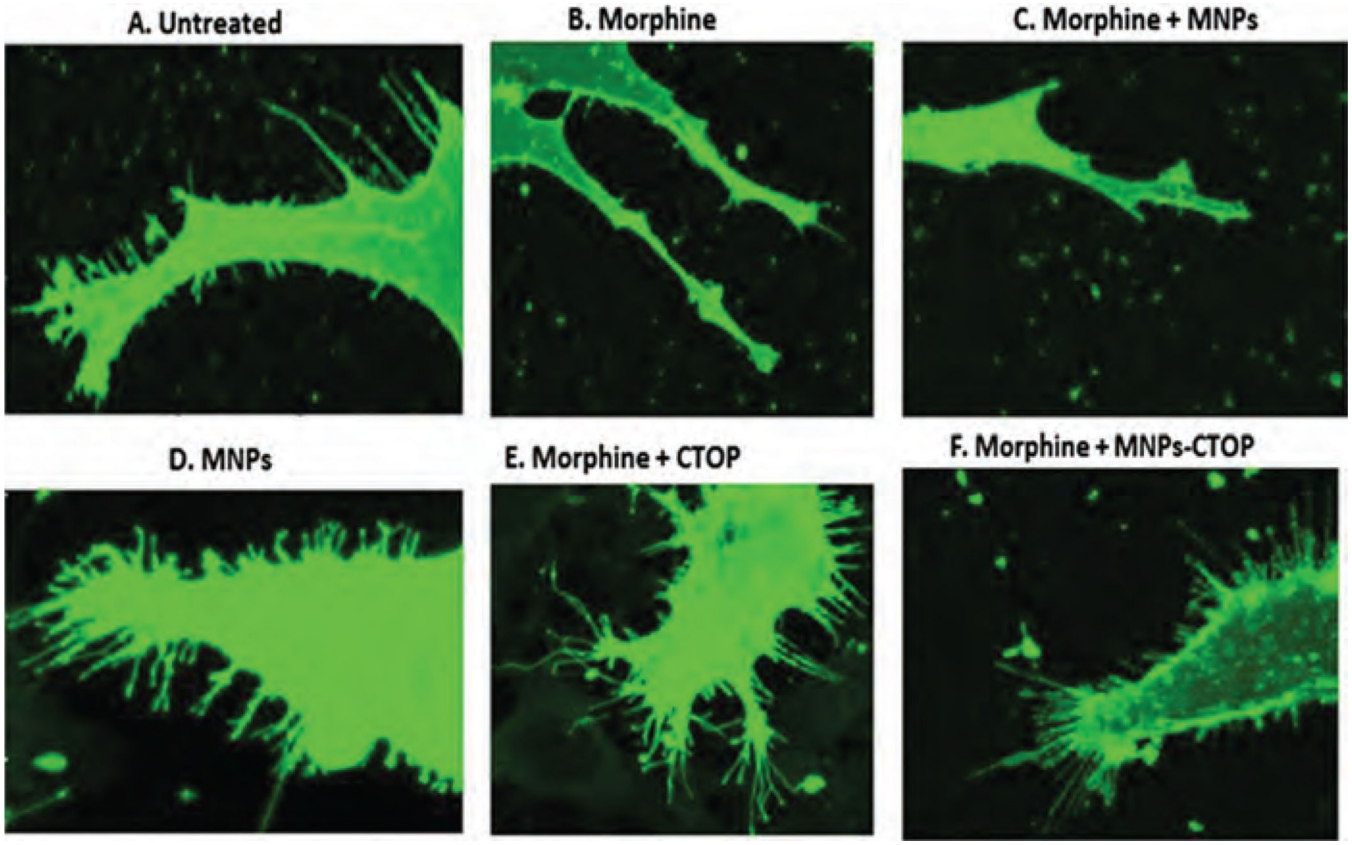

Figure 6.

Confocal microscopy to evaluate the efficacy of MNPs bound CTOP on morphine induced neuropathogenesis: Free (E) and MNP bound CTOP (F) prevents the morphine induced spinal degradation in neuroblastoma cells, SK-N-MC (B).

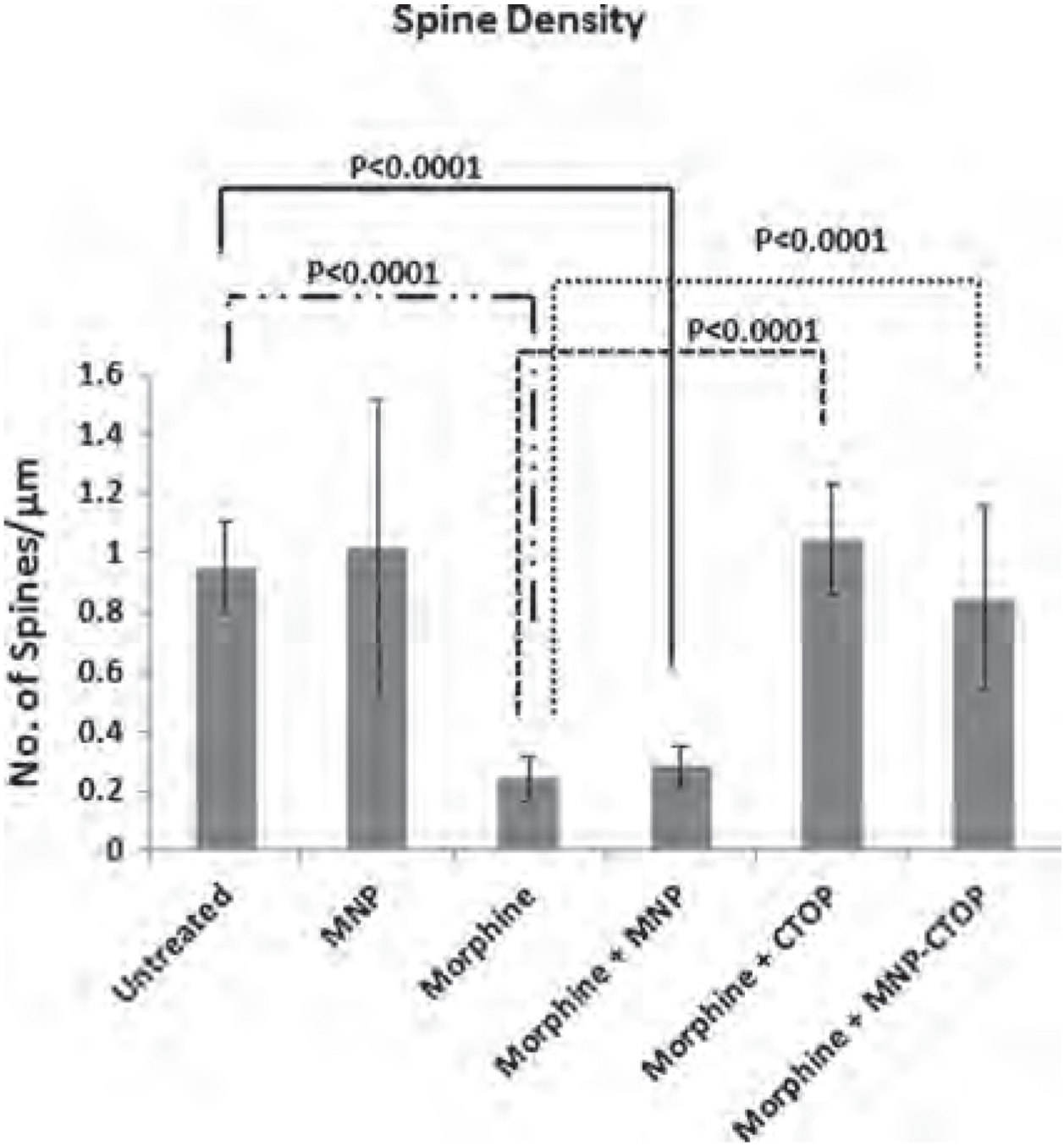

Figure 7.
Spinal density (No. of spines/µm dendritic length) of SK-N-MC showing morphine induced spinal degeneration and effect of Free and MNP bound CTOP on prevention of this degradation.

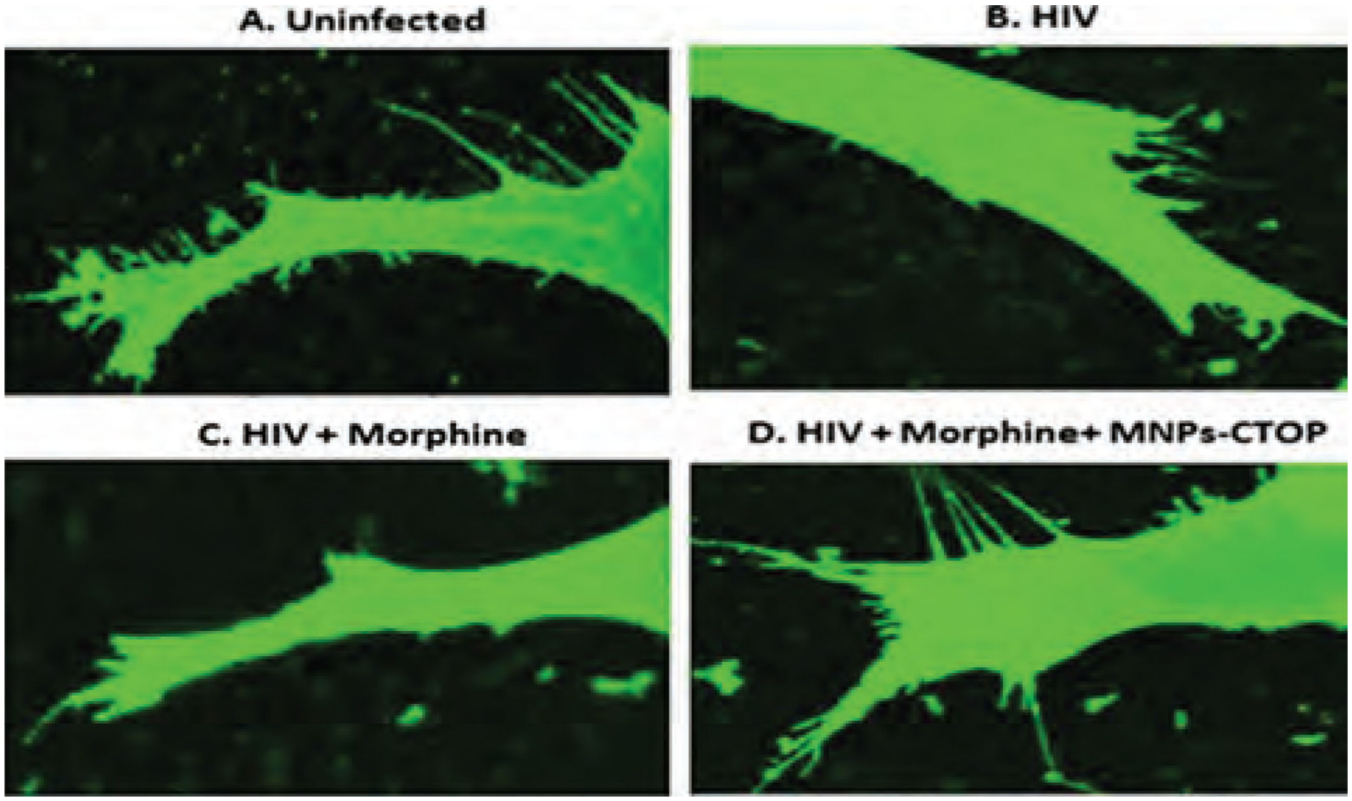

Figure 8.

Confocal microscopy to evaluate the efficacy of MNPs bound CTOP on morphine and HIV co-infection induced neuropathogenesis: MNP bound CTOP (D) prevents the spinal degradation in HIV-infected, morphine co-treated neuroblastoma cells, SK-N-MC.

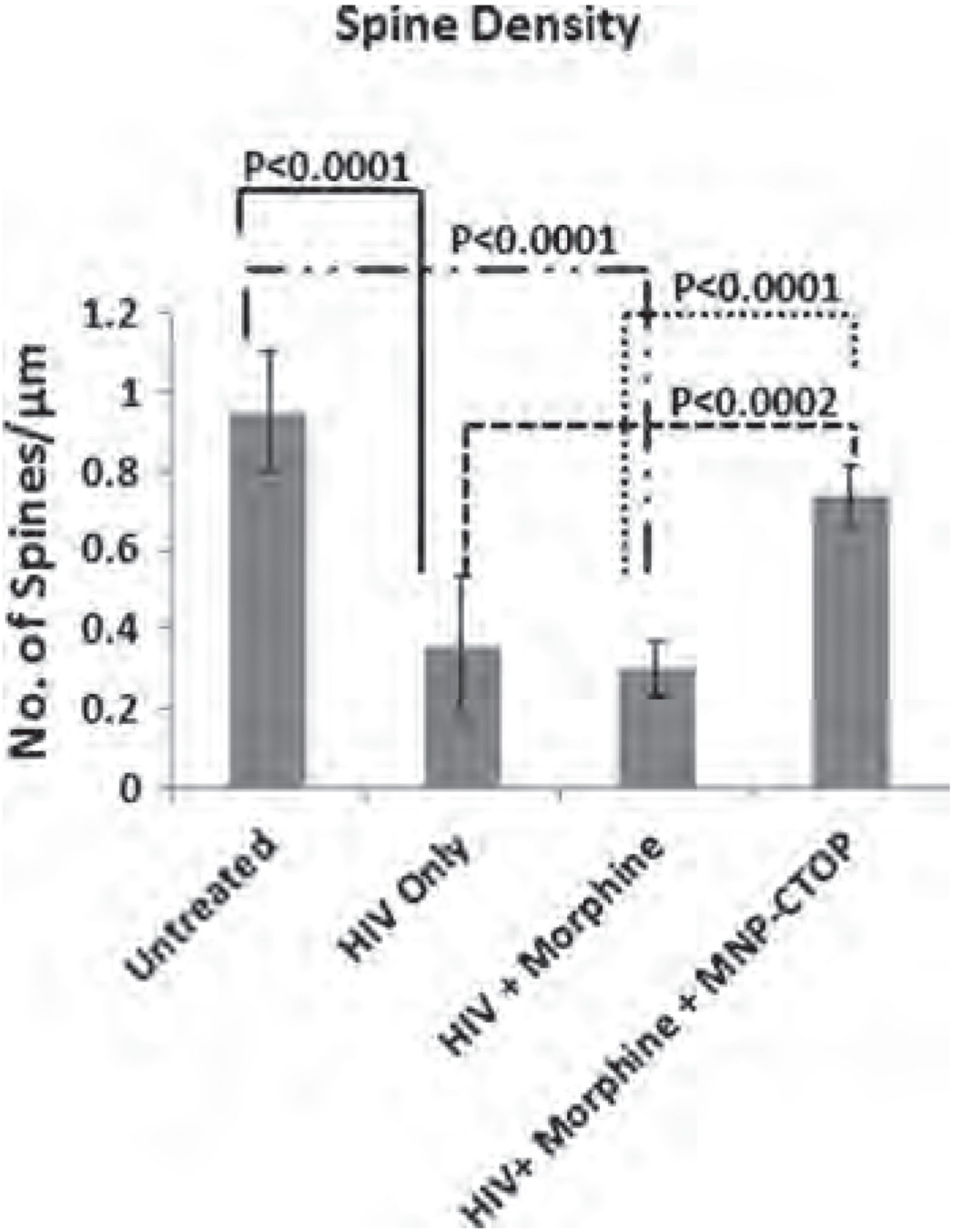

Figure 9.

Spinal density (No. of spines/µm dendritic length) of SK-N-MC showing morphine and HIV co-infection induced spinal degeneration and effect of MNP bound CTOP on prevention of this degradation.

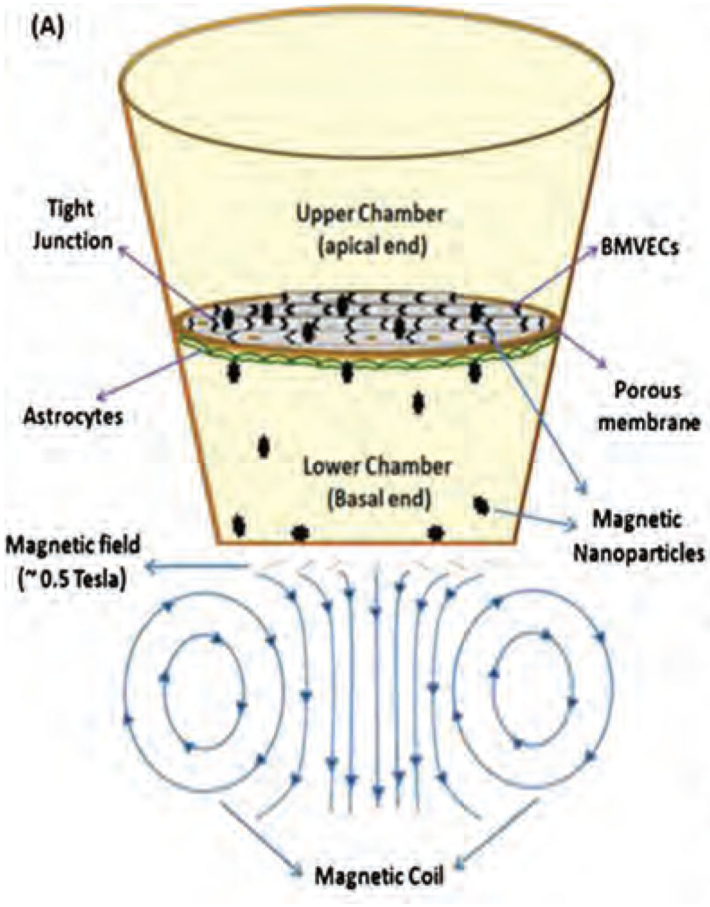

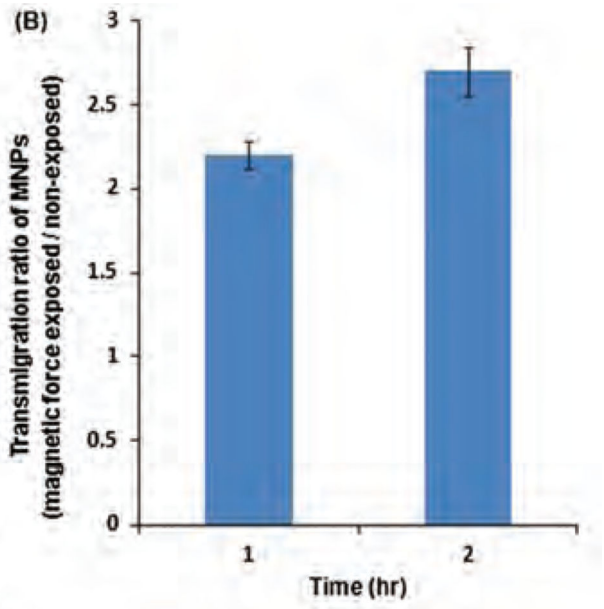

(C)

TEER Values (Ω/cm^2)	Magnetic Force	No force	Untreated
Before treatment	207 ± 8	199 ± 19	202 ± 7
After treatment	201 ± 11	202 ± 6	214 ± 14

Figure 10.

Proof-of-principle for enhanced transmigration of MNPs across *in vitro* BBB: (A) *In-vitro* BBB model of external magnetic force-driven transendothelial delivery of MNPs. (B) Transendothelial migration ratio of MNPs exposed and non-exposed to magnetic force. (C) TEER values of the *in vitro* BBB model before and after treatment of MNPs in the presence and absence of external magnetic force.